
Time Series Causal Discovery via Context-Conditioned and Causality-Augmented Pretraining

Biao Ouyang, Tengxue Zhang, Zhihao Zhuang, Yang Shu*, Chenjuan Guo, Bin Yang
 East China Normal University
 {bouyang, txzhang, zhuangzhihao}@stu.ecnu.edu.cn
 {yshu, cjguo, byang}@dase.ecnu.edu.cn

Abstract

Causal discovery from time series is critical for many real-world applications, such as tracing the root causes of anomalies. Existing approaches typically rely on dataset-specific optimization, making it difficult to transfer their causal discovery capabilities to new time series governed by diverse causal mechanisms. In this paper, we propose **PTCD**, a novel **Pretraining** framework for **Time-series Causal Discovery**, which improves cross-task generalization through context-conditioned modeling and transferable causal augmentation. To model complex temporal causal dependencies, PTCD employs a dual-scale iterative attention mechanism to capture window-level causal relationships, and a Gaussian mixture with a context-level routing mechanism to handle heterogeneous exogenous distributions. To further address distribution shifts across causal graphs, PTCD adopts a pretraining paradigm on synthetic datasets that integrates intervention-based learning and a causal mixup strategy, promoting stable causal discovery and stronger generalization. Extensive experiments on multiple real-world out-of-distribution (OOD) datasets demonstrate that PTCD excels in both causal discovery and root cause identification.

1 Introduction

Accurate causal discovery from observed time series is fundamental to many real-world applications. Causal analysis can reveal the drivers of stock price fluctuations [20] and the factors influencing river water levels [42]. It also facilitates identifying the sources of system failures and tracing how these failures propagate [12, 27], thereby enabling actionable insights and more robust decision-making.

As shown in Figure 1a, recent end-to-end causal discovery methods generalize poorly across different causal mechanisms and require costly per-dataset optimization, especially for time series with complex temporal dependencies. We therefore propose a pretraining paradigm that learns transferable causal discovery capabilities from diverse time series and causal graphs, enabling stronger generalization to new time series and supports accurate causal graph recovery in both zero-shot settings and with lightweight fine-tuning. However, building a generalizable pretraining framework for time series causal discovery faces two main challenges.

Challenge 1: *Inherent complexity of temporal causal dependencies.* As shown in Figure 1b, channel 3 at time t is influenced by channel 1 at $t - 2$, which in turn is influenced by channel 2 at $t - 4$. This reveals an iterative, cascading dependency across time steps. Existing methods [5, 12] inadequately capture such iterative cross-window interactions. This suggests that reliable temporal causal discovery requires modeling dependencies beyond individual windows. Furthermore, in structural causal models, observed time series (endogenous variables) are influenced not only by other endogenous variables but also by unobserved factors (exogenous variables). Since exogenous distributions vary across

*Corresponding author.

time series and causal structures, existing methods [31, 12] assuming a fixed Gaussian prior lack the flexibility to model diverse causal mechanisms.

Challenge 2: Lack of causality-aware generalization under distribution shifts. Real-world time series often undergo distribution shifts caused by changing environments or system dynamics, leading to out-of-distribution (OOD) scenarios. Therefore, a robust causal discovery model should generalize beyond the training distribution. However, existing methods fail to account for both the diversity of individual series and the variability of causal structures across different series. Additionally, in causal discovery, distinguishing between correlation and causation is crucial [32]. As shown in Figure 1b, both channel 3 at time t ($x_{3,t}$) and channel 2 at $t - 1$ ($x_{2,t-1}$) are influenced by channel 1 at $t - 2$, which induces correlation between them. However, this does not imply a direct causal link from $x_{2,t-1}$ and $x_{3,t}$. What truly matters is determining whether a causal relationship exists. Unfortunately, existing deep learning methods struggle to transfer this causal reasoning capability to unseen time series and causal graphs.

For **Challenge 1**, we propose a *hierarchical context-conditioned temporal causal discovery modeling approach*, which learns window-level representations at multiple scales and captures the distributions of exogenous variables in time series. Our framework features two key components: (1) *Dual-scale iterative representation enhancement*, which employs an attention-based mechanism to iteratively model both intra-window and inter-window dependencies, capturing fine-grained causal dynamics within windows while accounting for coarse-grained long-range causal propagation across windows; and (2) *Context-conditioned exogenous variable estimation*, which employs an adaptive mixture-of-Gaussians model with routing to approximate exogenous variable distributions in a context-conditioned manner, thereby enhancing the robustness of causal discovery across diverse time series.

For **Challenge 2**, we propose *generalizable causal learning with causal augmentation* to strengthen the model’s perception of causal relationships and improve its OOD robustness. Specifically, the *causal pretext task* introduces interventions into time series, breaking spurious correlations and providing strong signals for learning more generalizable causal structures. By treating the prediction of the intervened window as a pretext task, the model is encouraged to exploit discrepancies across varying time series and acquire transferable causal discovery capabilities. Furthermore, *Time series causal mixup* operates by jointly mixing latent representations and their associated causal graphs, generating augmented sequences with diverse causal strengths and dependency patterns. This not only enriches the training data with diverse causal scenarios but also compels the model to generalize beyond previously observed correlation structures. In summary, our contributions are as follows:

- We propose a novel pretraining paradigm for time-series causal discovery that can rapidly adapt to new time series and causal graphs.
- We introduce a hierarchical context-conditioned temporal causal discovery modeling that captures both inter-window and intra-window dependencies in individual time series, while flexibly handling context-conditioned exogenous noises across multiple series.

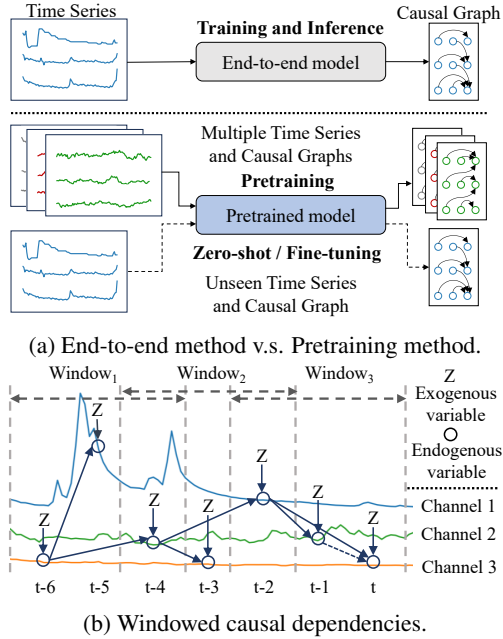


Figure 1: **(a)** End-to-end vs. pretraining paradigm: end-to-end models adopt dataset-specific optimization, while pretrained models learn from multiple time series and causal graphs, enabling zero-shot inference or fine-tuning on unseen time series/graphs. **(b)** Intra- and inter-window causal dependencies in multivariate time series x . Solid lines denote causal dependencies, while dashed lines indicate spurious correlations.

- We develop a generalizable causal pretraining strategy that employs intervention-based pretext tasks to break spurious correlations and reveal causal invariance in time series, alongside a causal mixup to achieve smoother gradients and improved robustness.
- Experiments on multiple real-world datasets show that PTCD consistently outperforms existing methods in both causal discovery and root cause identification.

2 Related Work

Causal Discovery for Time Series. Granger causality-based methods [11, 7] assume that if past values of X improve the prediction of future values of Y , then X is a Granger cause of Y . This idea has been extended with various neural architectures: cLSTM [44] leverages RNNs to infer Granger causal structures; TCDF [28] utilizes attention-based CNNs for interpretable causal discovery; GVAR [24] adopts a vector autoregressive model with generalized coefficient matrices to increase modeling flexibility; and CUTS [5, 6] learns a sparse causal adjacency matrix directly from data. However, these methods share a key limitation: they do not explicitly model endogenous errors or exogenous noise,

which restricts their applicability in practical scenarios. In contrast, Structural Causal Model (SCM) approaches explicitly characterize functional relationships among endogenous variables and account for exogenous influence: Varlingam [14] combines a non-Gaussian instantaneous causality with vector autoregressive dynamics; TiMINo [34] assumes that exogenous variables are independent over time; AERCA [12] uses an autoencoder to model both causal relationships and the distribution of exogenous variables. However, existing methods largely ignore distribution shifts, limiting their ability to generalize time series causal discovery across multiple datasets. To address these gaps, we leverage a causal pretext task to uncover causal relationships in temporal sequences and causal mixup to generate diverse dependency patterns, thereby improving OOD generalization for causal discovery.

Pre-trained Causal Discovery. Recent efforts have integrated causal discovery into pre-trained models [21, 16]. CaML [30] formulates personalized effect prediction as a meta-task for zero-shot generalization; Cond-FiP [23] dynamically infers structural causal models via a Fixed-Point Approach [36]; and CInA [49] learns transferable causal representations from unlabeled data, enabling zero-shot inference without fine-tuning. However, these methods do not explicitly capture temporal causality. CP [41] mitigates this by learning window-based causal graphs via supervised training across four architectures, yet it overlooks key temporal properties such as multi-scale dependencies and exogenous variable effects (see Table 1). To overcome these limitations, we leverage dual-scale attention to capture inter-window and intra-window temporal dependencies, and context-conditioned exogenous estimation to model the distribution of exogenous variables in each time series.

3 Problem Formulation

We consider a multivariate time series $\mathbf{x} = \{x_{1:T,i}\}_{i=1}^C$ with C channels, where $x_{1:T,i}$ denotes the length- T sequence for channel i . Following AERCA [12], we adopt the Granger Causality framework and assume causal sufficiency, no instantaneous effects, and time-invariant causal relations. For structural identifiability, we assume that the system satisfies the causal minimality [46] and follows a continuous nonlinear Additive Noise Model [33]. Under these assumptions, the data generation process is modeled as a time-invariant structural causal model (SCM):

$$x_{t,i} = g_i \left(\sum_{k=0}^{n-1} \sum_{j=1}^C G_{t-n+k,j,i} \cdot f_{k,j,i}(x_{t-n+k,j}) \right) + Z_{i,t}, \quad (1)$$

where n is the maximum time lag, $\mathbf{G} \in \mathbb{R}^{n \times C \times C}$ is the causal graph, and $G_{t-n+k,j,i}$ indicates the impact of channel j at time $t-n+k$ on $x_{t,i}$. The operator \cdot denotes scalar multiplication, and the

Table 1: Comparison of causal discovery methods. The symbol \checkmark indicates that a component is incorporated, while \times denotes its absence. Fine-grained and coarse-grained denote intra- and inter-window dependency, respectively. Exogenous refers to modeling of exogenous variables, and Generalization indicates the ability to handle unseen time series under different causal mechanisms.

Methods	Fine-grained	Coarse-grained	Exogenous	Generalization
CDMI [11]	\checkmark	\times	\times	\times
CUTS [5]	\checkmark	\times	\times	\times
TCDF [28]	\checkmark	\checkmark	\times	\times
CP [41]	\times	\checkmark	\times	\checkmark
AERCA [12]	\checkmark	\times	\checkmark	\times
PTCD	\checkmark	\checkmark	\checkmark	\checkmark

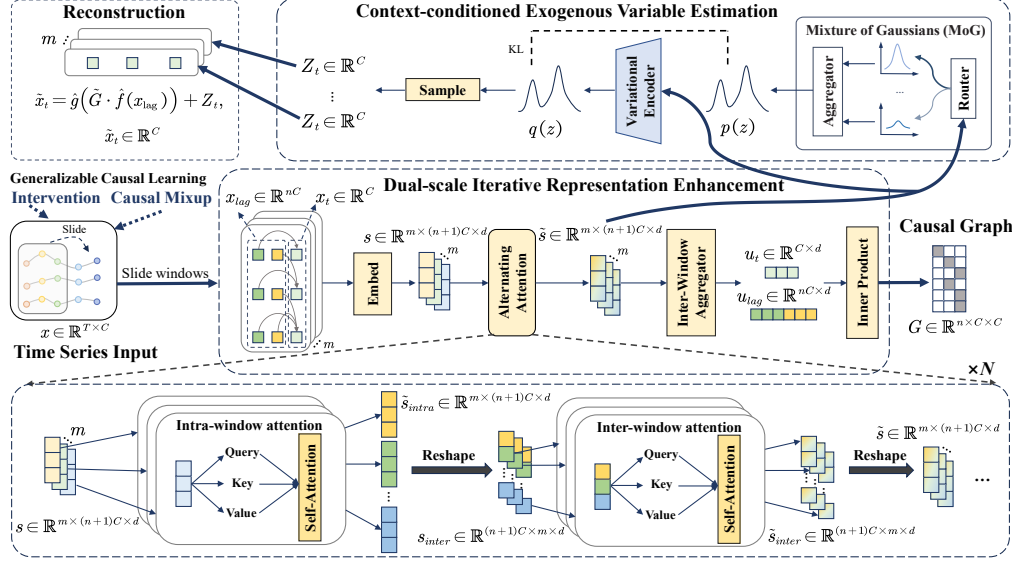


Figure 2: Overview of the hierarchical context-conditional temporal causal discovery framework, comprising: (1) Dual-scale Iterative Representation Enhancement, and (2) Context-conditioned exogenous variable estimation. The model’s generalization is further improved via transferable causality-augmented pretraining, incorporating intervention pretext task and causal mixup strategies.

functions $g_i(\cdot)$ and $f_{k,j,i}(\cdot)$ are nonlinear transformations of the past observations, and $Z_{i,t}$ is an exogenous noise term for channel i at time t .

In this work, we focus on pretraining a causal discovery model $G = F_\theta(x)$ that acquires transferable causal discovery capability. The learned model is expected to generalize to unseen time series and enable the discovery of causal graphs that are not observed during pretraining. Moreover, we further transfer the pretrained model to real-world settings for causal discovery and root cause identification.

4 Methodology

We propose **PTCD**, a generalizable framework for time series causal discovery with context-conditioned modeling and causality-augmented pretraining (Figure 2). To capture complex temporal dependencies and diverse exogenous influences, we introduce a **hierarchical context-conditioned causal discovery framework**. The dual-scale iterative representation enhancement module segments time series into sliding windows and alternates intra-window and inter-window attention to refine temporal representations. An inter-window aggregator then produces past and current node embeddings, whose inner products estimate the window causal graph. To model heterogeneous exogenous variables, the context-conditioned exogenous variable estimation module adopts a routing-based mixture-of-Gaussians prior and reconstructs the current series from the estimated causal graph and past observations. To improve generalization, we introduce **transferable causal learning with causal augmentation**. The intervention pretext task performs interventions on the generative process of time series and formulates a prediction task for the intervened window, thereby eliminating spurious correlations and enabling stable causal discovery across different environments. causal mixup regularizes causal dependencies by jointly interpolating latent representations and causal graphs. Finally, PTCD reconstructs time series by jointly modeling causal structure, endogenous dynamics, and exogenous factors, enabling interpretable and transferable causal discovery.

4.1 Hierarchical Context-Conditional Temporal Causal Discovery Framework

Dual-scale Iterative Representation Enhancement. To model complex causal dependencies over both short and long time scales, as shown in Figure 2, given a multivariate time series $x \in \mathbb{R}^{T \times C}$, we divide it into m windows of size $(n+1)$, yielding $x_{window} \in \mathbb{R}^{m \times (n+1) \times C}$. To model the data generation process of the current time step x_t , we represent each window as the concatenation of past observations $x_{lag} \in \mathbb{R}^{n \times C}$ and the current step $x_t \in \mathbb{R}^C$. We then embed x_{window} to

obtain the window representation $s_{intra} \in \mathbb{R}^{m \times (n+1)C \times d}$, where d represents the dimension of the embedding. Intra-window features capture local temporal dynamics, while inter-window relations provide global context. To jointly model these complementary scales, we propose an alternating attention mechanism that iteratively integrates features within and across windows. First, we apply self-attention within each window. The sequence s is projected into Q_{intra}^s , K_{intra}^s , and V_{intra}^s , and compute the intra-window representation as:

$$\tilde{s}_{intra} = \text{Softmax}\left(Q_{intra}^s (K_{intra}^s)^\top / \sqrt{d_k}\right) V_{intra}^s. \quad (2)$$

Next, we perform inter-window self-attention to capture dependencies across windows. Specifically, the $\tilde{s}_{intra} \in \mathbb{R}^{m \times (n+1)C \times d}$ is reshaped as $s_{inter} \in \mathbb{R}^{(n+1)C \times m \times d}$, projected into Q_{inter}^s , K_{inter}^s , and V_{inter}^s , and processed as:

$$\tilde{s}_{inter} = \text{Softmax}\left(Q_{inter}^s (K_{inter}^s)^\top / \sqrt{d_k}\right) V_{inter}^s. \quad (3)$$

The inter-window output \tilde{s}_{inter} is reshaped back and fed into the next iteration. Repeating this alternating process for N iterations progressively refines the representation, yielding the dual-scale enhanced representation $\tilde{s} \in \mathbb{R}^{m \times (n+1)C \times d}$. We then apply an inter-window aggregator over \tilde{s} to obtain node features $u \in \mathbb{R}^{(n+1)C \times d}$ for window causal graph construction. Following the partition of x_{lag} and x_t , we split u into past nodes u_{lag} and the current nodes u_t . Finally, we encode u_{lag} and u_t separately, and compute their inner product to estimate the link probability matrix \tilde{G} :

$$\begin{aligned} u &= \text{Aggregator}(\tilde{s}), \quad \tilde{G} = \text{MLP}(u_{lag})\text{MLP}(u_t)^T, \\ u &\in \mathbb{R}^{(n+1)C \times d}, \quad u_{lag} \in \mathbb{R}^{nC \times d}, \quad u_t \in \mathbb{R}^{C \times d}. \end{aligned} \quad (4)$$

Here, \tilde{G} is a binary matrix indicating the presence or absence of causal links. The causal graph is trained to align the estimated link probability matrix \tilde{G} with its ground-truth matrix G as:

$$\text{BCE}(G, \tilde{G}) = -G \cdot \log(\tilde{G}) - (1 - G) \cdot \log(1 - \tilde{G}). \quad (5)$$

Context-conditioned Exogenous Variable Estimation. Considering the diversity of time series and their underlying causal mechanisms, the distributions of exogenous variables can vary substantially across datasets. Therefore, we propose a context-conditioned approach that leverages the dual-scale enhanced representation \tilde{s} as contextual input to estimate exogenous variable distributions. According to Equation (1), we define a data-generating distribution $p(D)$ that jointly encapsulates the underlying causal structure and the influence of exogenous factors:

$$x \sim p(D) = \int_G \int_z p(D | G, z) \cdot p(G) \cdot p(z) dz dG. \quad (6)$$

Here, a sample x is generated by first drawing from the prior distribution of exogenous variable $p(z)$ and the causal structure distribution $p(G)$, and then iteratively generating data through the data-generating mechanism $p(D|G, z)$.

In time series, noise and external disturbances often exhibit diverse patterns, reflecting heterogeneous exogenous influences. Therefore, a single shared Gaussian prior is insufficient to model such variability. To address this, we model the exogenous prior as a context-conditioned Gaussian mixture, where the mixing coefficients $\pi \in \mathbb{R}^K$ are generated from the enhanced representation \tilde{s} via a routing mechanism. The means μ and variances Σ of the K Gaussian components are learnable parameters:

$$\pi = \text{Router}(\tilde{s}), p(z) = \sum_{k=1}^K \pi_k \mathcal{N}(z | \mu_k, \Sigma_k), \sum_{k=1}^K \pi_k = 1, \quad (7)$$

where $\text{Router}(\cdot)$ maps the context \tilde{s} to mixing weights, and \mathcal{N} denotes the Gaussian probability density function.

We employ a variational encoder to approximate the posterior distribution $q(z)$ of the exogenous variables conditioned on the temporal representation \tilde{s} . Using the reparameterization trick, we sample the exogenous variable Z_t from $q(z)$ at each time step t . According to Eq. 1, the sampled variable Z_t is then incorporated into the reconstruction of the current time series x_t , together with the predicted causal graph \tilde{G} , and the lagged endogenous variables x_{lag} . In this manner, both exogenous influences

and the causal dependencies are explicitly modeled, ensuring that the learned representations are consistent with a structural causal model. The reconstruction of x_t is formulated as:

$$\tilde{x}_t = \tilde{g} \left(\tilde{G}_p \cdot \tilde{f}(x_{lag}) \right) + Z_t, \quad (8)$$

where $\tilde{g}(\cdot)$ and $\tilde{f}(\cdot)$ denote multi-layer perceptrons. We use the reconstruction error $\|x_t - \tilde{x}_t\|_2$ as the supervision signal for both pre-training and fine-tuning.

To regularize the latent space, we introduce a KL divergence term between the learned posterior distribution $q(z)$ and the assumed prior mixture Gaussian distribution $p(z)$:

$$\mathcal{L}_{KL}(p(z) \parallel q(z)) = \int p(\mathbf{z}) \log \frac{p(\mathbf{z})}{q(\mathbf{z})} d\mathbf{z}, \quad (9)$$

4.2 Transferable Causal Learning with Causal Augmentation

Intervention Pretext Task. Time series data often exhibit autocorrelation and interdependencies, where past values influence the present, and multivariate series may involve cross-channel causality. Relying solely on observational data can confuse correlation and causality, making it difficult to distinguish between causal graphs within the same Markov equivalence class [18, 45]. Interventions on variables, by actively altering the underlying data-generating mechanisms, provide additional information that enhances causal identifiability.

We propose an intervention pretext task that uses interventions to facilitate causal structure learning. Specifically, we randomly select a time interval $[t_1, t_2]$ from the time series x and replace the observation at t_1 with a randomly sampled value. Based on the underlying causal dynamics, we then iteratively propagate this intervention to compute the intervened segment $(x'_{t_1}, \dots, x'_{t_2})$, replacing the original segment $(x_{t_1}, \dots, x_{t_2})$ to obtain a modified series x^{do} . By examining segmented windows of x^{do} , we identify those inconsistent with the causal structure to derive binary ground-truth intervention labels. To enhance generalization and encourage the model to capture stable causal dependencies, we train it to predict the window in which an intervention occurs. We formulate intervention detection as a classification task for intervention detection:

$$\mathcal{L}_{do_window} = \sum_{i=1}^m \left(-h_i \log(\hat{h}_i) - (1 - h_i) \log(1 - \hat{h}_i) \right), \quad (10)$$

where h_i and \hat{h}_i denote the ground-truth and predicted intervention labels for window i , respectively.

Furthermore, Theorem 4.1 shows that optimizing the proposed intervention detection objective is equivalent to identifying the true causal mechanisms. The proof is provided in Appendix A.1.

Theorem 4.1. (Causal Identifiability via Intervention Detection) *Let $P_{obs}(\mathbf{x})$ denote the observational distribution induced by the true SCM, and $P_{int}(\mathbf{x})$ denote the interventional distribution where a subset of variables $\mathbf{x}_{\mathcal{I}}$ (e.g., a time window) is replaced by samples from a noise or marginal proposal distribution $Q(\mathbf{x}_{\mathcal{I}})$. The optimal discriminator D^* that minimizes the intervention classification loss is monotonically dependent on the true causal mechanism $P(\mathbf{x}_{\mathcal{I}} \mid Pa(\mathbf{x}_{\mathcal{I}}))$. Consequently, optimizing \mathcal{L}_{do_window} necessitates the model to learn the true underlying causal structure and the associated conditional dependencies.*

To preserve semantic consistency under interventions, we apply contrastive learning to align the representation u^{do} of the intervened series x^{do} with the representation u of the original x using Eq. 4:

$$\mathcal{L}_{do_contrast} = - \sum_{i=1}^{(n+1)C} \log \frac{\exp(\text{sim}(u^{do,+}, u_i)/\tau)}{\sum_{j=1}^{(n+1)C} \exp(\text{sim}(u_j^{do}, u_i)/\tau)}, \quad (11)$$

where τ is a temperature parameter, $\text{sim}(\cdot, \cdot)$ is the similarity function, and $u^{do,+}$ denotes the positive pair of u_i from the same node in the window causal graph. We jointly optimize the intervention detection objective and contrastive objective, i.e., $\mathcal{L}_{do} = \mathcal{L}_{do_window} + \mathcal{L}_{do_contrast}$ to enhance causal discovery capability. The reconstruction loss on x^{do} is computed following Eq. 8.

Time Series Causal Mixup. To improve the generalization of the causal discovery framework, we propose a time series causal mixup strategy for temporal causal discovery. This operation smooths the solution space, yielding more stable and continuous estimates of edge existence. Specifically, we randomly sample two time series from the training dataset, each with latent embedding \tilde{s}^i and its corresponding causal relation G^i . We then construct mixed samples as:

$$\tilde{s}^m = \lambda_1 \tilde{s}^1 + \lambda_2 \tilde{s}^2, \quad G^m = \lambda_1 G^1 + \lambda_2 G^2, \quad (12)$$

where the mixing coefficient λ_i is drawn from a Beta distribution. By blending samples from diverse time series and varying causal graphs, time series causal mixup achieves a smoother optimization landscape during training, enhancing the transferability of causal dependency modeling.

We further present Theorem 4.2, which suggests that causal mixup enforces the learned causal probabilities to be transferable and physically consistent, avoiding the artifacts introduced by input-space interpolation. The proof is provided in Appendix A.2. Since function smoothness is closely related to generalization [40, 47], PTCD achieves transferable causal discovery capability.

Theorem 4.2. (Geodesic Consistency of Causal Probability) *Under Assumption A.2, linear interpolation in the latent space \mathcal{S} approximates a geodesic interpolation on the data manifold \mathcal{M} . Minimizing the Mixup empirical risk objective, which penalizes the discrepancy between the network prediction $\hat{G}(s^{mix})$ and the interpolation target $\lambda G(x_1) + (1 - \lambda)G(x_2)$ under a bounded loss ϵ , inherently imposes an implicit gradient penalty proportional to the Frobenius norm of the Jacobian, $\mathcal{O}(\|\nabla_s \hat{G}(s)\|_F^2)$. This bounds the local Lipschitz constant of the causal mapping, regularizing the Jacobian field to be smooth along the transport path and ensuring stable causal graph discovery.*

Following Eq. 5, we compute the binary cross-entropy loss $\text{BCE}(G^m, \tilde{G}^m)$ between the estimated link probability matrix \tilde{G} and the mixup link probability matrix G^m .

4.3 Causal Learning and Root Cause Identification

Pretraining Phase. During pretraining, we generate synthetic datasets by iteratively simulating time series from causal graphs (see Appendix B.1) to train the model. Given a time series x , the objective function consists of several components: the reconstruction loss \mathcal{L}_{recon} , the causal graph loss \mathcal{L}_G , the KL divergence loss \mathcal{L}_{KL} , the intervention loss \mathcal{L}_{do} . The overall pre-training loss is defined as:

$$\mathcal{L}_{pre} = \mathcal{L}_{recon} + \lambda_G \mathcal{L}_G + \lambda_{KL} \mathcal{L}_{KL} + \lambda_{do} \mathcal{L}_{do}, \quad (13)$$

where $\lambda_G, \lambda_{KL}, \lambda_{do}$ are the corresponding weighting coefficients. The reconstruction loss \mathcal{L}_{recon} is computed over two types of input, the original series, the intervened series, and is defined as $\mathcal{L}_{recon} = \|x_t - \tilde{x}_t\|_2 + \|x_t^{do} - \tilde{x}_t^{do}\|_2$. The causal graph loss \mathcal{L}_G is computed over two types of input, the original series, the mixup series, and is defined as $\mathcal{L}_G = \text{BCE}(G, \tilde{G}) + \text{BCE}(G^m, \tilde{G}^m)$.

Fine-tuning Phase. During fine-tuning, we address two downstream tasks: *Causal Discovery* and *Root Cause Identification*. In real-world scenarios, the true data generation process is typically unavailable. Hence, we focus solely on the reconstruction loss with s_t , and the KL divergence loss \mathcal{L}_{KL} . The overall fine-tuning loss is as follows:

$$\mathcal{L}_{ft} = \|\tilde{s}_t - s_t\|_2 + \lambda_{KL} \mathcal{L}_{KL}. \quad (14)$$

For *Root Cause Identification*, following AERCA [12], we score exogenous variable abnormality to pinpoint root causes. We compute the mean (μ) and standard deviation (σ) of the exogenous distribution from normal data, and compute the root cause score as the z-score, $\text{score}_t = \min_{k=1}^K \left(\frac{Z_t - \mu_k}{\sigma_k} \right)$. We then adopt Streaming Peaks-Over-Threshold [39] for threshold selection.

5 Experiments

5.1 Experimental Design

Datasets. We construct a synthetic time series causal dataset (see Appendix B.1) for pretraining and fine-tune the model on two real-world tasks. *Causal Discovery.* We evaluate on the German river benchmark [42], which includes causal graphs from Eastern Germany (666 stations) and Bavaria (494

Table 2: Causal discovery results of AUROC on Eastern Germany river datasets, best in bold and second-best underlined.

Dataset \ Model	TCDF	CUTS+	VAR	Varlingam	Dynotears	PCMCI	CDMI	CP(Gru)	CP(Transformer)	PTCD
Close (3)	0.57	0.56	<u>0.81</u>	0.79	0.50	0.64	<u>0.81</u>	0.79	0.75	0.84
Close (5)	0.51	0.54	0.81	0.77	0.50	0.62	0.81	0.81	<u>0.83</u>	0.85
Root cause (3)	0.55	0.56	0.79	0.77	0.56	0.70	0.75	0.78	<u>0.84</u>	0.88
Root cause (5)	0.54	0.59	0.75	0.77	0.56	0.74	0.65	0.81	<u>0.84</u>	0.86
Random+1 (3)	0.72	0.56	0.80	<u>0.84</u>	0.52	0.83	0.82	0.82	0.82	0.87
Random+1 (5)	0.56	0.57	0.79	0.79	0.61	0.74	0.80	<u>0.84</u>	0.85	0.85
Confounder (3)	0.62	0.55	<u>0.71</u>	0.68	0.53	0.66	0.63	0.64	0.65	0.81
Confounder (5)	0.56	0.51	<u>0.72</u>	0.70	0.53	0.64	0.71	0.71	0.71	0.79
Random (3)	0.55	0.57	<u>0.82</u>	0.79	0.50	0.65	0.80	0.77	0.81	0.85
Random (5)	0.52	0.54	0.80	0.75	0.51	0.65	0.78	<u>0.83</u>	0.86	0.86
avg	0.57	0.56	0.78	0.77	0.53	0.69	0.76	0.78	0.80	0.85

Table 3: Results of root cause identification, best in bold.

Dataset	Model	Recall@1	Recall@3	Recall@5	Recall@10	Avg@10
MSDS	ϵ -Diagnosis	0.004±0.004	0.266±0.002	0.452±0.009	1.000±0.000	0.492±0.001
	RCD	0.412±0.048	0.573±0.010	0.984±0.001	1.000±0.000	0.821±0.012
	CIRCA	0.454±0.238	0.860±0.140	0.917±0.084	1.000±0.000	0.809±0.035
	AERCA	0.381±0.408	0.908±0.062	0.974±0.027	1.000±0.000	0.896±0.037
	PTCD	0.515±0.252	0.993±0.004	0.996±0.003	1.000±0.000	0.929±0.013
SWaT	ϵ -Diagnosis	0.075±0.179	0.125±0.217	0.125±0.217	0.375±0.383	0.180±0.194
	RCD	0.000±0.000	0.000±0.000	0.000±0.000	0.300±0.458	0.100±0.161
	CIRCA	0.000±0.000	0.000±0.000	0.000±0.000	0.300±0.458	0.100±0.161
	AERCA	0.220±0.111	0.290±0.088	0.330±0.048	0.455±0.044	0.342±0.052
	PTCD	0.300±0.132	0.450±0.107	0.450±0.137	0.475±0.141	0.440±0.105

stations), covering two variable types and five causal relation types: Close, Root Cause, Random+1, Confounder, and Random. The model is fine-tuned on Bavaria and evaluated on Eastern Germany. *Root Cause Identification.* We fine-tune and evaluate on two benchmarks. The SWaT dataset [25], collected from a scaled-down water treatment testbed under both normal and cyber-attack conditions, is widely used for intrusion detection in industrial control systems. The MSDS dataset [29], generated on an OpenStack-based distributed infrastructure, injects controlled faults to emulate anomalies in multi-source cloud environments. Dataset details are provided in Appendix B.1.

Evaluation Metrics. *Causal Discovery.* To avoid threshold tuning, we report the AUROC score [26, 13, 43, 28]. *Root Cause Identification.* Following prior work [15, 19, 48, 22, 12], we evaluate using recall at top- k , denoted as $Recall@K$. This metric measures the probability of correctly identifying root causes within the top- k highest root cause scores. Further details are in Appendix B.3.

Baselines. *Causal Discovery.* We evaluate representative methods spanning classical and modern paradigms. Classical approaches include PCMCI [35], Varlingam [14], Dynotears [31], VAR [2], CDMI [1], TCDF [28], CUTS+ [6]. Among recent pretraining methods, we compare with Causal Pretraining (CP) [41], which is implemented through both Transformer-based and GRU-based architectures. *Root Cause Identification.* We compare PTCD with four baselines: 1) ϵ -Diagnosis [38], 2) RCD [15], 3) CIRCA [19], and 4) AERCA [12].

5.2 Experimental Results

Causal Discovery. Table 2 presents the results for time series causal graph discovery, demonstrating that PTCD consistently outperforms all baselines across various types of causal relationships. This highlights the effectiveness of its dual-scale iterative representation enhancement and context-conditioned exogenous variables estimation in capturing complex causal dependencies. This approach enables the model to accurately identify true causal dependencies among time series while filtering out spurious correlations caused by confounders or environmental biases. For example, we observe that PTCD achieves strong causal discovery performance on the Eastern Germany river dataset, despite not being directly trained on it. Notably, compared to CP, our method demonstrates a significant improvement, with an average gain of 5%. These results confirm that PTCD acquires a generalizable mechanism for causal discovery through intervention-based modeling and causal mixup, ensuring robustness even under real-world distribution shifts.

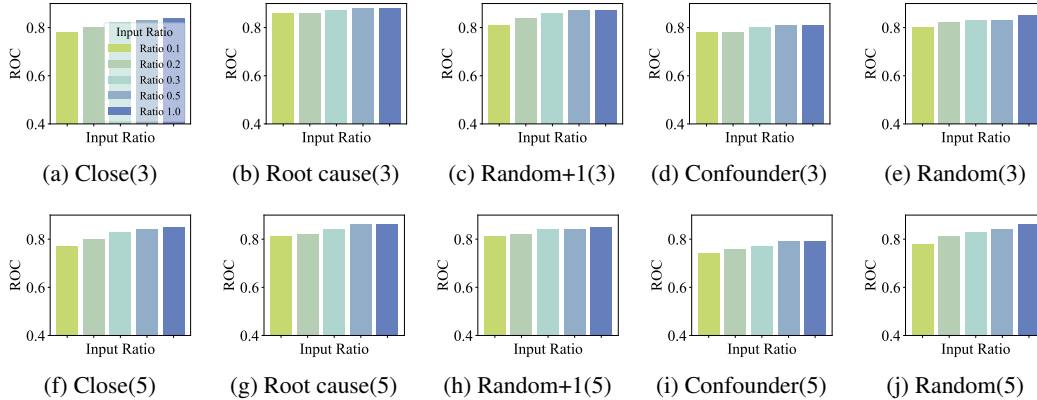


Figure 3: Results on the Eastern Germany river dataset (avg. length 3,143) under test input ratios of 10%, 20%, 30%, 50%, and 100%.

Table 4: Ablation study of causal discovery using the Eastern Germany river dataset. w/o inter, w/o intra, w/o exogenous, w/o causal mixup, w/o intervention represent removing the inter-window attention, intra-window attention, exogenous, causal mixup, and intervention, respectively.

Model \ Dataset	w/o inter	w/o intra	w/o exogenous	w/o causal mixup	w/o intervention	PTCD
Close (3)	0.83	0.82	0.80	0.83	0.80	0.84
Close (5)	0.84	0.82	0.81	0.83	0.81	0.85
Root cause (3)	0.86	0.84	0.82	0.86	0.83	0.88
Root cause (5)	0.85	0.84	0.82	0.85	0.83	0.86
Random+1 (3)	0.85	0.84	0.83	0.86	0.84	0.87
Random+1 (5)	0.83	0.83	0.82	0.83	0.81	0.85
Confounder (3)	0.79	0.79	0.78	0.80	0.75	0.81
Confounder (5)	0.78	0.76	0.75	0.77	0.74	0.79
Random (3)	0.84	0.84	0.81	0.83	0.82	0.85
Random (5)	0.85	0.84	0.83	0.84	0.83	0.86
avg	0.83	0.82	0.81	0.83	0.81	0.85

Root Cause Identification. Table 3 shows that PTCD achieves the best performance on real-world datasets in the root cause diagnosis task. Unlike AERCA, which primarily focuses on intra-window modeling, PTCD leverages a dual-scale iterative representation enhancement to capture both coarse-grained and fine-grained temporal patterns. This approach enhances the model’s ability to detect subtle variations over time, leading to superior performance in identifying the root cause of anomalies. Furthermore, the context-conditioned exogenous variable estimation boosts PTCD to adapt to the complex and often noisy conditions found in real-world data. According to the AC@1 metric, PTCD excels in accurately identifying the time series with the highest root cause score, demonstrating that incorporating intervention-based pre-training enables more stable detection of anomalous root causes even in the presence of dynamic shifts and external disturbances.

Ablation Studies. To assess the impact of different components in PTCD, we conduct an ablation study on inter-window attention, intra-window attention, mixture of Gaussians exogenous variables, causal mixup, and intervention. As shown in Table 4, each module contributes to the overall performance. Notably, removing exogenous variable estimation significantly reduces performance, highlighting the importance of learning context-conditioned distributions. Furthermore, the inclusion of intervention yields notable performance improvements, particularly in datasets where the root cause is confounded (Confounder (3) and Confounder (5)). This demonstrates that interventions help the model distinguish between spurious correlations and true causal relationships, enhancing the accuracy of causal graph prediction. Further ablation studies are in Appendix B.5.

Different Time Series Ratio. Figure 3 shows the impact of varying lengths of the input time series on performance. We find that using only 30% of the full sequence length yields results comparable to the complete input, while even 10% still provides reasonable results across all datasets. This shows

that PTCB remains effective under limited resources and efficient for causal discovery using reduced temporal inputs, making it suitable for real-world applications.

6 Conclusions

This paper introduces PTCB, a novel pretraining framework for generalizable time series causal discovery across diverse downstream tasks. To capture complex temporal dependencies, PTCB employs a dual-scale attention mechanism for both fine-grained local dynamics and long-range causal relationships, complemented by a context-conditioned Gaussian mixture to accommodate heterogeneous exogenous variable distributions flexibly. To handle distribution shifts, PTCB incorporates a causal mixup and intervention-based learning to achieve causal augmentation, promoting stable causal discovery and stronger generalization. Experiments on real-world OOD datasets show that PTCB outperforms existing methods in causal discovery and root cause identification, establishing it as a robust foundation for time series analysis.

References

- [1] Wasim Ahmad, Valentin Kasburg, Nina Kukowski, Maha Shadaydeh, and Joachim Denzler. Deep-learning based causal inference: A feasibility study based on three years of tectonic-climate data from moxa geodynamic observatory. *Earth and Space Science*, 11(10):e2023EA003430, 2024.
- [2] Charles K. Assaad, Emilie Devijver, and Éric Gaussier. Survey and evaluation of causal discovery methods for time series (extended abstract). In *IJCAI*, pages 6839–6844, 2023.
- [3] Albert-László Barabási and Réka Albert. Emergence of scaling in random networks. *Science*, 286(5439): 509–512, 1999.
- [4] Yoshua Bengio, Aaron C. Courville, and Pascal Vincent. Representation learning: A review and new perspectives. *IEEE TPAMI*, 35(8):1798–1828, 2013.
- [5] Yuxiao Cheng, Runzhao Yang, Tingxiong Xiao, Zongren Li, Jinli Suo, Kunlun He, and Qionghai Dai. CUTS: neural causal discovery from irregular time-series data. In *ICLR*, 2023.
- [6] Yuxiao Cheng, Lianglong Li, Tingxiong Xiao, Zongren Li, Jinli Suo, Kunlun He, and Qionghai Dai. Cuts+: High-dimensional causal discovery from irregular time-series. In *AAAI*, volume 38, pages 11525–11533, 2024.
- [7] Rainer Dahlhaus and Michael Eichler. Causality and graphical models in time series analysis. *Highly structured stochastic systems*, pages 115–137, 2003.
- [8] Paul Erdős and Alfréd Rényi. On random graphs. *Publicationes Mathematicae*, 6:290–297, 1959.
- [9] Wenbo Gong, Joel Jennings, Cheng Zhang, and Nick Pawlowski. Rhino: Deep causal temporal relationship learning with history-dependent noise. In *ICLR*, 2023.
- [10] Ian J. Goodfellow, Jean Pouget-Abadie, Mehdi Mirza, Bing Xu, David Warde-Farley, Sherjil Ozair, Aaron C. Courville, and Yoshua Bengio. Generative adversarial nets. In *nips*, pages 2672–2680, 2014.
- [11] Clive WJ Granger. Investigating causal relations by econometric models and cross-spectral methods. *Econometrica: journal of the Econometric Society*, pages 424–438, 1969.
- [12] Xiao Han, Saima Absar, Lu Zhang, and Shuhan Yuan. Root cause analysis of anomalies in multivariate time series through granger causal discovery. In *ICLR*, 2025.
- [13] Uzma Hasan, Emam Hossain, and Md. Osman Gani. A survey on causal discovery methods for I.I.D. and time series data. *Trans. Mach. Learn. Res.*, 2023, 2023.
- [14] Aapo Hyvärinen, Kun Zhang, Shohei Shimizu, and Patrik O. Hoyer. Estimation of a structural vector autoregression model using non-gaussianity. *J. Mach. Learn. Res.*, 11:1709–1731, 2010.
- [15] Azam Ikram, Sarthak Chakraborty, Subrata Mitra, Shiv Kumar Saini, Saurabh Bagchi, and Murat Kocaoglu. Root cause analysis of failures in microservices through causal discovery. In *NeurIPS*, 2022.
- [16] Nan Rosemary Ke, Silvia Chiappa, Jane X. Wang, Jörg Bornschein, Anirudh Goyal, Mélanie Rey, Theophane Weber, Matthew M. Botvinick, Michael Curtis Mozer, and Danilo Jimenez Rezende. Learning to induce causal structure. In *ICLR*, 2023.
- [17] Diederik P. Kingma and Jimmy Ba. Adam: A method for stochastic optimization. In *ICLR*, 2015.
- [18] Adam Li, Amin Jaber, and Elias Bareinboim. Causal discovery from observational and interventional data across multiple environments. *Advances in Neural Information Processing Systems*, 36:16942–16956, 2023.
- [19] Mingjie Li, Zeyan Li, Kanglin Yin, Xiaohui Nie, Wenchi Zhang, Kaixin Sui, and Dan Pei. Causal inference-based root cause analysis for online service systems with intervention recognition. In *KDD*, pages 3230–3240, 2022.
- [20] Shuqi Li, Yuebo Sun, Yuxin Lin, Xin Gao, Shuo Shang, and Rui Yan. Causalstock: Deep end-to-end causal discovery for news-driven multi-stock movement prediction. In *NeurIPS*, 2024.
- [21] Lars Lorch, Scott Sussex, Jonas Rothfuss, Andreas Krause, and Bernhard Schölkopf. Amortized inference for causal structure learning. In *nips*, 2022.
- [22] Meng Ma, Jingmin Xu, Yuan Wang, Pengfei Chen, Zonghua Zhang, and Ping Wang. Automap: Diagnose your microservice-based web applications automatically. In *WWW*, pages 246–258, 2020.

- [23] Divyat Mahajan, Jannes Gladrow, Agrin Hilmkil, Cheng Zhang, and Meyer Scetbon. Zero-shot learning of causal models. *CoRR*, abs/2410.06128, 2024.
- [24] Ricards Marcinkevics and Julia E. Vogt. Interpretable models for granger causality using self-explaining neural networks. In *ICLR*, 2021.
- [25] Aditya P. Mathur and Nils Ole Tippenhauer. Swat: a water treatment testbed for research and training on ICS security. In *2016 International Workshop on Cyber-physical Systems for Smart Water Networks, CySWater@CPSWeek 2016*, pages 31–36, 2016.
- [26] Raha Moraffah, Paras Sheth, Mansooreh Karami, Anchit Bhattacharya, Qianru Wang, Anique Tahir, Adrienne Raglin, and Huan Liu. Causal inference for time series analysis: problems, methods and evaluation. *Knowl. Inf. Syst.*, 63(12):3041–3085, 2021.
- [27] Lokesh Nagalapatti, Ashutosh Srivastava, Sunita Sarawagi, and Amit Sharma. Robust root cause diagnosis using in-distribution interventions. In *ICLR*, 2025.
- [28] Meike Nauta, Doina Bucur, and Christin Seifert. Causal discovery with attention-based convolutional neural networks. *Mach. Learn. Knowl. Extr.*, 1(1):312–340, 2019.
- [29] Sasho Nedelkoski, Jasmin Bogatinovski, Ajay Kumar Mandapati, Soeren Becker, Jorge Cardoso, and Odej Kao. Multi-source distributed system data for ai-powered analytics. In *ESOC*, volume 12054 of *Lecture Notes in Computer Science*, pages 161–176, 2020.
- [30] Hamed Nilforoshan, Michael Moor, Yusuf H. Roohani, Yining Chen, Anja Surina, Michihiro Yasunaga, Sara Oblak, and Jure Leskovec. Zero-shot causal learning. In *NeurIPS*, 2023.
- [31] Roxana Pamfil, Nisara Sriwattanaworachai, Shaan Desai, Philip Pilgerstorfer, Konstantinos Georgatzis, Paul Beaumont, and Bryon Aragam. DYNOTEARS: structure learning from time-series data. In *AISTATS*, volume 108 of *Proceedings of Machine Learning Research*, pages 1595–1605, 2020.
- [32] Judea Pearl and Dana Mackenzie. *The Book of Why: The New Science of Cause and Effect*. Basic Books, New York, 2018.
- [33] Jonas Peters, Dominik Janzing, and Bernhard Schölkopf. Identifying cause and effect on discrete data using additive noise models. In *AISTATS*, volume 9 of *JMLR Proceedings*, pages 597–604, 2010.
- [34] Jonas Peters, Dominik Janzing, and Bernhard Schölkopf. Causal inference on time series using restricted structural equation models. In *NeurIPS*, pages 154–162, 2013.
- [35] Jakob Runge, Peer Nowack, Marlene Kretschmer, Seth Flaxman, and Dino Sejdinovic. Detecting and quantifying causal associations in large nonlinear time series datasets. *Science advances*, 5(11):eaau4996, 2019.
- [36] Meyer Scetbon, Joel Jennings, Agrin Hilmkil, Cheng Zhang, and Chao Ma. Fip: a fixed-point approach for causal generative modeling. *CoRR*, abs/2404.06969, 2024.
- [37] Bernhard Schölkopf, Francesco Locatello, Stefan Bauer, Nan Rosemary Ke, Nal Kalchbrenner, Anirudh Goyal, and Yoshua Bengio. Toward causal representation learning. *Proc. IEEE*, 109(5):612–634, 2021.
- [38] Huasong Shan, Yuan Chen, Haifeng Liu, Yunpeng Zhang, Xiao Xiao, Xiaofeng He, Min Li, and Wei Ding. ϵ -diagnosis: Unsupervised and real-time diagnosis of small- window long-tail latency in large-scale microservice platforms. In *WWW*, pages 3215–3222, 2019.
- [39] Alban Siffer, Pierre-Alain Fouque, Alexandre Termier, and Christine Largouët. Anomaly detection in streams with extreme value theory. In *SIGKDD*, pages 1067–1075. ACM, 2017.
- [40] Jure Sokolic, Raja Giryes, Guillermo Sapiro, and Miguel R. D. Rodrigues. Robust large margin deep neural networks. *IEEE Trans. Signal Process.*, 65(16):4265–4280, 2017.
- [41] Gideon Stein, Maha Shadaydeh, and Joachim Denzler. Embracing the black box: Heading towards foundation models for causal discovery from time series data. *CoRR*, abs/2402.09305, 2024.
- [42] Gideon Stein, Maha Shadaydeh, Jan Blunk, Niklas Penzel, and Joachim Denzler. Causalrivers - scaling up benchmarking of causal discovery for real-world time-series. In *ICLR*, 2025.
- [43] Xiangyu Sun, Oliver Schulte, Guiliang Liu, and Pascal Poupart. NTS-NOTEARS: learning nonparametric dbns with prior knowledge. In *International Conference on Artificial Intelligence and Statistics*, volume 206 of *Proceedings of Machine Learning Research*, pages 1942–1964, 2023.

- [44] Alex Tank, Ian Covert, Nicholas Foti, Ali Shojaie, and Emily B Fox. Neural granger causality. *IEEE Transactions on Pattern Analysis and Machine Intelligence*, 44(8):4267–4279, 2021.
- [45] Jin Tian and Judea Pearl. Causal discovery from changes. In *UAI*, pages 512–521, 2001.
- [46] Sumanth Varambally, Yian Ma, and Rose Yu. Discovering mixtures of structural causal models from time series data. In *ICML*, 2024.
- [47] Vikas Verma, Alex Lamb, Christopher Beckham, Amir Najafi, Ioannis Mitliagkas, David Lopez-Paz, and Yoshua Bengio. Manifold mixup: Better representations by interpolating hidden states. In *ICML*, volume 97 of *Proceedings of Machine Learning Research*, pages 6438–6447, 2019.
- [48] Guangba Yu, Pengfei Chen, Hongyang Chen, Zijie Guan, Zicheng Huang, Linxiao Jing, Tianjun Weng, Xinmeng Sun, and Xiaoyun Li. Microrank: End-to-end latency issue localization with extended spectrum analysis in microservice environments. In *WWW*, pages 3087–3098, 2021.
- [49] Jiaqi Zhang, Joel Jennings, Agrin Hilmkil, Nick Pawlowski, Cheng Zhang, and Chao Ma. Towards causal foundation model: on duality between optimal balancing and attention. In *ICML*, 2024.

A Proofs

A.1 Proofs of Intervention Pretext Task

In this section, we provide the theoretical guarantee for the effectiveness of our proposed Intervention Pretext Task. We formally prove that minimizing the intervention detection loss is equivalent to estimating the true conditional causal mechanism, thereby enabling the model to identify the true parents in the causal graph.

Proof. The Intervention Pretext Task is formulated as a binary classification problem. Let $y = 1$ denote samples from the observational distribution P_{obs} , and $y = 0$ denote samples from the interventional distribution P_{int} . The objective is to minimize the binary cross-entropy loss \mathcal{L}_{do} :

$$\mathcal{L}_{do} = -\mathbb{E}_{\mathbf{x} \sim P_{\text{obs}}}[\log D(\mathbf{x})] - \mathbb{E}_{\mathbf{x} \sim P_{\text{int}}}[\log(1 - D(\mathbf{x}))], \quad (15)$$

where $D(\mathbf{x})$ represents the probability that \mathbf{x} is from the observational distribution.

According to the classical result in density ratio estimation [10], for fixed distributions P_{obs} and P_{int} , the optimal discriminator $D^*(\mathbf{x})$ that minimizes this loss is given by:

$$D^*(\mathbf{x}) = \frac{P_{\text{obs}}(\mathbf{x})}{P_{\text{obs}}(\mathbf{x}) + P_{\text{int}}(\mathbf{x})}. \quad (16)$$

Now, consider the factorization of the joint probability based on the causal graph G . Let the intervention be performed on a specific variable (in window) x_i at time t , replacing it with a value drawn from $Q(x_i)$. The observational distribution factors according to the causal Markov condition:

$$P_{\text{obs}}(\mathbf{x}) = P(x_i | Pa(x_i)) \cdot \prod_{j \neq i} P(x_j | Pa(x_j)). \quad (17)$$

The interventional distribution, where the causal mechanism of x_i is replaced by $Q(x_i)$ while other mechanisms remain invariant, factors as:

$$P_{\text{int}}(\mathbf{x}) = Q(x_i) \cdot \prod_{j \neq i} P(x_j | Pa(x_j)). \quad (18)$$

Substituting these factorizations into Eq. (16), the terms for all non-intervened variables $\prod_{j \neq i} P(x_j | Pa(x_j))$ are common to both the numerator and the denominator and thus cancel out. The optimal discriminator simplifies to:

$$D^*(\mathbf{x}) = \frac{P(x_i | Pa(x_i))}{P(x_i | Pa(x_i)) + Q(x_i)} = \sigma \left(\log \frac{P(x_i | Pa(x_i))}{Q(x_i)} \right), \quad (19)$$

where $\sigma(\cdot)$ is the sigmoid function.

Since $Q(x_i)$ is a known proposal distribution (e.g., mixture Gaussian distribution), and $\sigma(\cdot)$ is a strictly monotonic function, the output of the optimal discriminator $D^*(\mathbf{x})$ is determined solely by the true conditional probability $P(x_i | Pa(x_i))$.

Therefore, to minimize the loss \mathcal{L}_{do} , the model D is forced to approximate D^* . This implies that the model must accurately estimate the conditional likelihood $P(x_i | Pa(x_i))$. An accurate estimation of this term is only possible if the model correctly identifies the true parent set $Pa(x_i)$ and models the correct functional relationship. Relying on spurious correlations would yield a suboptimal estimate of the conditional density, resulting in a higher loss. This proves that the intervention pretext task provides a sufficient signal for recovering the causal parents and discovering the underlying causal relationships. \square

A.2 Proofs of Time Series Causal Mixup

Let $x_t \in \mathcal{X} \subseteq \mathbb{R}^d$ denote the observed system state. The dynamics are governed by a structural equation $x_{t+1} = f^*(x_t) + \epsilon$, where f^* is the ground-truth mechanism. We focus on estimating the **Causal Probability Matrix**, defined as the Jacobian $G(x) := J_{f^*}(x) = \frac{\partial f^*}{\partial x} \in \mathbb{R}^{d \times d}$.

Standard mixup operates in the input space \mathcal{X} . However, physical observations usually lie on a low-dimensional manifold $\mathcal{M} \subset \mathcal{X}$ embedded in the high-dimensional ambient space. A convex combination $\lambda x_1 + (1 - \lambda)x_2$ often falls off the manifold \mathcal{M} , leading to physically invalid states where the causal mechanism f^* is undefined.

To resolve the geometric inconsistency, we leverage the concept of causal representation learning.

Definition A.1 (Latent Causal Embedding). We assume there exists a latent space $\mathcal{S} \subseteq \mathbb{R}^k$ and an encoder function $\phi : \mathcal{X} \rightarrow \mathcal{S}$. While ϕ is implemented as a neural network, we assume it acts as a smooth embedding on the support of the data manifold \mathcal{M} . Specifically, $\phi|_{\mathcal{M}}$ is injective and preserves the topological structure of the causal mechanisms.

This definition aligns with the *Manifold Hypothesis*, where deep networks learn to unfold complex curved manifolds into flatter representations [4].

Assumption A.2 (Linearity of Mechanisms in Disentangled Space). Following the principle of Independent Causal Mechanisms (ICM) [37], we assume that in the ideal disentangled latent space \mathcal{S} , the dynamics $g(s)$ (where $s = \phi(x)$) are governed by simpler, smoother mechanisms compared to the ambient space. Locally, the evolution in \mathcal{S} can be well-approximated by linear transitions.

Geodesic Consistency via Causal Mixup. We propose performing mixup in \mathcal{S} . Let $s_1 = \phi(x_1)$ and $s_2 = \phi(x_2)$. The mixed state is $s^{mix} = \lambda z_1 + (1 - \lambda)z_2$.

1. Geodesic Interpretation. Since ϕ acts as a smooth embedding (Definition A.1), the image of the data manifold $\phi(\mathcal{M})$ in \mathcal{S} is locally homeomorphic to Euclidean space. A straight line segment in \mathcal{S} defined by $\gamma_s(\lambda) = \lambda s_1 + (1 - \lambda)s_2$ corresponds to a curve $\gamma_x(\lambda) = \phi^\dagger(\gamma_s(\lambda))$ in the original space \mathcal{X} , where ϕ^\dagger denotes the pseudo-inverse or decoder mapping. Because ϕ unfolds the manifold, the curve $\gamma_x(\lambda)$ approximates the **geodesic** (shortest path) between x_1 and x_2 constrained to lie on \mathcal{M} . Unlike input mixup, which creates off-manifold samples, Causal Mixup generates valid physical states along this geodesic.

2. Jacobian Dynamics and Chain Rule. Let the dynamics in the latent space be described by $s_{t+1} = g(s_t)$. The relationship between the observed causal probability $G(x)$ and the latent mechanism is given by the chain rule:

$$G(x) = \frac{\partial f^*}{\partial x} = J_{\phi^\dagger}(s) \cdot \frac{\partial g}{\partial s} \cdot J_\phi(x) \quad (20)$$

where J_ϕ and J_{ϕ^\dagger} are the Jacobians of the encoder and decoder, respectively.

3. Regularization via Mixup and Jacobian Smoothing. Causal Mixup optimizes the model by minimizing the mixup loss between the network’s predicted causal probability and the linear interpolation target. The empirical risk objective can be formally defined as:

$$\mathcal{L}_{mixup} = \mathbb{E}_\lambda \left[\left\| \hat{G}(s^{mix}) - (\lambda G(x_1) + (1 - \lambda)G(x_2)) \right\|_F^2 \right] \quad (21)$$

where $s^{mix} = s_2 + \lambda(s_1 - s_2)$ is the mixed latent state, $\hat{G}(\cdot)$ is the neural network predictor, and $G(\cdot)$ represents the target causal mechanism.

To rigorously quantify the implicit regularization effect of this objective, we employ Taylor’s Theorem with the Lagrange remainder. By defining the perturbation direction as $\Delta s = s_1 - s_2$, the mixed state can be rewritten as $s^{mix} = s_2 + \lambda\Delta s$. Applying a first-order Taylor expansion to the network output yields:

$$\hat{G}(s_2 + \lambda\Delta s) = \hat{G}(s_2) + \lambda \nabla_s \hat{G}(s_2) \Delta s + R_2 \quad (22)$$

where R_2 represents the Lagrange remainder. Minimizing the objective \mathcal{L}_{mixup} forces the Taylor expansion of the network output to match the linear interpolation of the targets. This optimization process yields an implicit gradient penalty proportional to the Frobenius norm of the Jacobian, denoted as $\mathcal{O}(\|\nabla_s \hat{G}(s)\|_F^2)$, with the approximation error tightly controlled by the spectral norm of the Hessian.

Formally, if the mixup loss is bounded by a small value ϵ , the Hessian norm is bounded by $\mathcal{O}(\epsilon)$. This implies that the Jacobian $\nabla_s \hat{G}(s)$ is locally constant up to an $\mathcal{O}(\epsilon)$ variation along the interpolation path. Consequently, minimizing the mixup loss inherently bounds the local Lipschitz constant of

the causal mapping \hat{G} . Under Assumption A.2, this mathematical equivalence ensures the global smoothness of the causal field and effectively prevents structural instability in the inferred causal graphs.

4. Handling ReLU Networks (Piecewise Linearity). While we assumed smoothness, modern neural networks (MLPs with ReLU) are piecewise linear functions. The input space is partitioned into polytopes where the network is an affine transformation. Within each polytope, ϕ is strictly linear, and its Jacobian J_ϕ is constant. Causal Mixup interpolates across these regions. By enforcing the linearity of the output G with respect to the convex combination in \mathcal{S} , we effectively regularize the transitions across the boundaries of these linear regions, ensuring that the global causal field remains continuous and smooth.

Causal Mixup acts as a regularizer that enforces the *Parallel Transport* of the causal mechanism along the data manifold. This minimizes the curvature of the learned causal field, leading to better generalization and structural identifiability compared to input-space interpolation. Therefore, time series causal Mixup not only enables a valid mixup process but also boosts the model’s generalization performance.

B Experiments

B.1 Details of Datasets

Synthetic Datasets.

Referring the data generation process of RHINO [9], we generate diverse time series and causal graphs. For the synthetic data pipeline, we construct the synthetic datasets using a four-step simulation process designed to capture diverse causal mechanisms. The procedure is defined as follows:

1. **Topology Generation:** We generate random Erdős–Rényi (ER) or Scale-Free (SF) graphs [8, 3] to specify the underlying lagged causal relationships between variables.
2. **Exogenous Noise Sampling:** For each time series, the exogenous variables were drawn from random Gaussian Mixture Models (GMMs) to introduce non-Gaussian complexity.
3. **Temporal Simulation:** We sample initial starting conditions and simulate the temporal progression of the system following Eq. 1 with additive noise. The functional relationships governing the dynamics were modeled using MLPs with two hidden layers (64 units each) and ReLU activation functions.
4. **Stabilization:** A burn-in period was simulated and subsequently discarded to ensure the time series reached a stable, stationary regime.

For dataset specifications, we generate datasets across multiple axes of variation. The specific configurations are detailed below:

- **System Size and Topology:** The number of nodes varies from 5 to 40. Both ER and SF graph structures are utilized.
- **Sequence Length:** Each generated time series has a length of $T = 100$ steps, obtained after removing an initial burn-in period of 100 steps.
- **Training Dataset:** The training corpus is designed to cover a wide range of structural variations. We generate 1,000 distinct causal graphs for each node count. For each causal graph, we simulate 5 independent multivariate time series. This yields a total dataset size of 180,000 time series.
- **Validation and Test Datasets:** The validation and test datasets each contain 370 time series, along with their corresponding ground-truth causal graphs for evaluation. Notably, these causal graphs are strictly disjoint from the training dataset.
- **Interventional Data:** To facilitate the learning of the intervention pretext task, we generate interventional samples for the training dataset. Specifically, we first sample a start time t_1 and an end time t_2 . We then randomly resample the specific treatment variables at time t_1 . Conditioned on this intervention, we iteratively generate the sequence over the interval $(t_1, t_2]$. Finally, we assign a binary label to each window indicating whether it contains an intervention.

Real-world Benchmark. CausalRiver [42] treats river flow measurements from monitoring stations as a time series dataset with inherent causal structure. It covers two regions in Germany: the eastern German territory (666 measuring stations) and Bavaria (494 stations). The dataset spans from 2019 to 2023 with a temporal resolution of 15 minutes. Importantly, CausalRiver includes both normal hydrological conditions and extreme events such as heavy rainfall and large-scale precipitation, enabling the study of causal dynamics under diverse environmental scenarios. The dataset is categorized into five types based on the characteristics of their underlying causal structures:

- **Random:** All connected subgraphs with three or five nodes, covering the entire dataset and full diversity of benchmark conditions.
- **Close:** Connected subgraphs whose edges have a maximum geographic (Euclidean) distance of 0.3; by excluding long-range connections, causal effects are expected to be more pronounced. This set is fully contained within Random.
- **Random + 1:** Connected subgraphs with two or four nodes, combined with one additional isolated node. To avoid confounding, the isolated nodes are drawn from coastal or border regions where disconnected nodes naturally occur.
- **Root cause:** Connected subgraphs with three or five nodes in which each node has at most one parent, forming chain-like structures. This setting is useful for root-cause analysis [15] and is fully contained within Random.
- **Confounder:** Subgraphs with four or six nodes containing a single node with multiple children (rarely observed in cases such as river splits). The multi-child node is then removed to simulate permanent hidden confounding.

Root Cause Identification Datasets. SWaT [25] is a dataset collected from a testbed that simulates a real-world water treatment plant. It comprises data from 51 sensors in the critical infrastructure system during continuous operation, including both normal operating conditions and attack scenarios within the water treatment process. MSDS (Multi-Source Distributed System) [29] is developed on an OpenStack testbed and serves as a dataset for AIOps (Artificial Intelligence for IT Operations). Instances of fault injections in this system are labeled as anomalies. More detail are provided in Table 5.

Table 5: Details of Root Cause Identification Datasets.

Dataset	Training Time Steps	Test Sequences	Avg. Sequence Length	Avg. # of Root Causes
SWaT (51)	49,500	20	51	13.35
MSDS (10)	29,268	4,255	21	3.05

B.2 More Details of Baselines

We provide detailed descriptions of the baseline methods used for comparison in both Causal Discovery and Root Cause Identification tasks.

Causal Discovery Baselines. We evaluate representative methods spanning classical statistical approaches and modern deep learning paradigms.

- **PCMCI** [35]: A constraint-based algorithm optimized for time-series data. It first selects preliminary parents using PC-algorithm-based selection and then estimates the causal graph using momentary conditional independence tests to control the false positive rate. It effectively handles time lags and strong autocorrelation.
- **VarLINGAM** [14]: A linear non-Gaussian acyclic model extended for autoregressive processes. It assumes the data generating process is linear with non-Gaussian noise and utilizes independent component analysis to identify the causal structure and time-lagged causal effects.
- **DYNOTEARS** [31]: A score-based method that formulates structural learning as a continuous optimization problem. It extends the NOTEARS framework to dynamic causal networks by minimizing a penalized loss function subject to acyclicity constraints, allowing for the simultaneous learning of intra-slice and inter-slice dependencies.

- **VAR** [2]: A classic statistical model that captures the linear interdependencies among multiple time series. In the context of causal discovery, Granger Causality is inferred based on the non-zero coefficients of the fitted autoregressive matrices.
- **CDMI** [1]: A method based on Causal Discovery with Mutual Information. It estimates the causal probability between time series variables by quantifying the mutual information shared between past values of potential parents and current values of the target, often utilizing non-parametric estimators to capture non-linear dependencies.
- **TCDF** [28]: A deep learning framework that uses attention-based CNNs. It learns a predictive model for each time series and interprets the internal attention parameters and variable importance scores to discover causal links and time delays.
- **CUTS+** [6]: An improved version of the CUTS framework designed for non-stationary time series. It employs a latent causal discovery approach where a Granger-causality-inspired graph is learned jointly with a data augmentation strategy to handle distribution shifts and improve robustness.
- **Causal Pretraining (CP)** [41]: A self-supervised pretraining framework designed to learn causal representations from time series. It reconstructs masked sub-series to capture temporal dependencies. To evaluate the impact of the backbone architecture, we compare two variants:
 - **CP-Trans**: Implements the standard CP framework using a Transformer-based backbone to capture long-range dependencies via self-attention mechanisms.
 - **CP-GRU**: Implements the CP framework using a gated recurrent unit backbone, focusing on sequential recurrent modeling.

Root Cause Identification Baselines. To evaluate the effectiveness of PTCD in identifying root causes of anomalies, we compare it with four established methods:

- **ϵ -Diagnosis** [38]: A statistical approach that locates root causes by analyzing the correlation changes between variables. It performs pairwise significance tests (e.g., standard deviation and correlation shifts) between normal and abnormal periods to construct an anomaly propagation graph and rank potential root causes.
- **RCD** [15]: A framework that integrates causal structure learning with anomaly attribution. It learns a partial causal graph from data and analyzes the invariance of conditional distributions. Nodes corresponding to intervention targets are identified as root causes.
- **CIRCA** [19]: A method that leverages domain knowledge to construct structural causal graphs. It identifies root causes by modeling the residuals of causal mechanisms; specifically, it detects nodes that exhibit significant distribution shifts in their conditional probabilities during the anomaly window.
- **AERCA** [12]: A reconstruction-based method that models causal dependencies and exogenous variables using an Autoencoder framework. It posits that anomalies are generated by perturbations in exogenous factors. AERCA attributes root causes by measuring the magnitude of the reconstruction error associated with the exogenous noise terms of each variable.

B.3 More Details of Metrics on Root Cause Identification

Given a multivariate time series \mathcal{X} , the $Recall@K$ is defined as:

$$Recall@K = \frac{1}{|\mathcal{X}|} \sum_{x_i \in \mathcal{X}} \frac{|V_{x_i}^{(RC)} \cap \{R_{x_i}[k] \mid k = 1, 2, \dots, K\}|}{\min(K, |V_{x_i}^{(RC)}|)}, \quad (23)$$

where $R_{x_i}[k]$ indicates the time series at the k -th rank for the channel x_i , and $V_{x_i}^{(RC)}$ indicates a set of root cause variables over the whole channel x_i . Note that if a time series receives multiple exogenous interventions, it only counts as one root cause time series in $V_{x_i}^{(RC)}$. We further compute the overall performance by computing the average $Recall@K$, denoted as $Avg@K = \frac{1}{K} \sum_{k=1}^K Recall@k$.

B.4 Implementation Details

We first pretrain PTC D using the Adam optimizer [17] with a learning rate of 10^{-3} . We apply early stopping with a patience of 30 epochs to prevent overfitting. The loss weights λ_G , λ_{KL} and λ_{do} are set to 0.6. The model consists of 4 alternating attention blocks, and the number of Gaussian components K is set to 10. For fine-tuning in both the causal discovery task and the root cause identification task, we use a learning rate of 10^{-4} , and keep λ_{KL} fixed at 0.6. All experiments are implemented in PyTorch and conducted on an NVIDIA A800 80GB GPU. Following AERCA [12], data preprocessing is standardized across datasets using a MinMax scaler. To improve computational efficiency, we downsample the SWaT dataset every 10 seconds and the MSDS dataset every 5 time steps. The code and datasets are available at <https://anonymous.4open.science/r/PTCD-D4E3>.

B.5 More Ablation Study

To investigate the impact of different components on root cause identification, we conduct an ablation study focusing on inter-window attention, intra-window attention, mixture-of-Gaussians modeling of exogenous variables, causal mixup, and intervention. As shown in Table 6, we find that the intervention mechanism achieves superior performance in identifying root causes. This gain is attributed to the fact that interventions provide the model with information across diverse environments, enabling it to filter out spurious correlations, learn more accurate causal relationships, and enhance overall robustness. Furthermore, when the mixture-of-Gaussians constraint on exogenous variables is removed, PTC D exhibits a notable drop in performance, demonstrating the importance of instance-specific exogenous variable estimation for effective root cause identification.

Table 6: Ablation studies on Root Cause Localization. w/o inter, w/o intra, w/o exogenous, w/o causal mixup, w/o intervention represent removing the inter-window attention, intra-window attention, exogenous, causal mixup, and intervention, respectively.

Dataset	Model	Recall@1	Recall@3	Recall@5	Recall@10	Avg@10
MSDS	w/o inter	0.452	0.792	0.910	1.000	0.492
	w/o intra	0.498	0.801	0.910	1.000	0.835
	w/o exogenous	0.227	0.697	0.893	1.000	0.694
	w/o causal mixup	0.500	0.792	0.993	1.000	0.842
	w/o intervention	0.296	0.798	0.900	1.000	0.728
	PTCD	0.515	0.993	0.996	1.000	0.929
SWaT	w/o inter	0.200	0.350	0.350	0.455	0.351
	w/o intra	0.250	0.375	0.375	0.450	0.360
	w/o exogenous	0.100	0.150	0.250	0.350	0.205
	w/o causal mixup	0.250	0.330	0.450	0.455	0.342
	w/o intervention	0.150	0.220	0.330	0.375	0.252
	PTCD	0.300	0.450	0.450	0.475	0.440

B.6 Efficiency Analysis

Table 7: Efficiency comparison across different paradigms on the causalriver dataset.

Model	Paradigm	Params (K)	Inference Time	GPU Mem (MB)	CPU Mem (MB)	avg. AUROC
TCDF	End-to-End Causal	0.12	17.19 s	2.00	460.45	0.57
CUTS+	End-to-End Causal	8.23	14.19 s	2.00	293.36	0.56
PTCD (zero-shot)	Pre-trained Causal	877.24	0.01 s	1236.00	504.08	0.74
PTCD (fine-tune)	Pre-trained Causal	877.24	3.59 s	1236.00	504.08	0.85

To provide a comprehensive efficiency profile, we evaluate the parameters, inference time, and memory usage across different paradigms. As shown in Table 7, although PTC D introduces a moderate parameter overhead due to pre-training, its fine-tuned variant achieves the best overall performance, at the expense of increased inference time compared to the zero-shot setting. This demonstrates a favorable trade-off: zero-shot PTC D offers exceptional efficiency, while the fine-tuned variant delivers superior predictive accuracy, all while retaining rapid inference capabilities.

B.7 Parameter Sensitivity Analysis

We conduct a hyperparameter sensitivity analysis with respect to the loss weights λ_G , λ_{KL} , and λ_{do} , which correspond to the causal graph loss, the KL-divergence loss, and the intervened loss, respectively, as well as the number of Gaussian components K . All experiments are performed on synthetic datasets. As shown in Figure 4, PTCD achieves optimal causal discovery performance when λ_G , λ_{KL} , and λ_{do} are set to 0.6. This indicates that causal graph prediction, the modeling of exogenous variables, and intervention mechanisms play a significant role in the generalization capability of the learned causal discovery. Additionally, the number of Gaussian components also influences the model’s generalization performance to a certain degree.

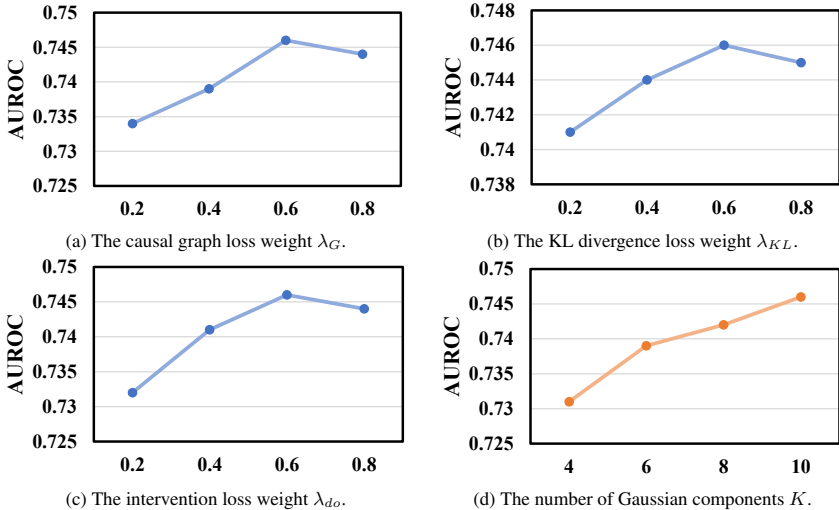


Figure 4: The effect of parameter λ_G , λ_{KL} , λ_{do} , and K on synthetic datasets for time-series causal discovery.

C Limitations

While PTCD demonstrates strong generalization capabilities in time series causal discovery and root cause identification, it has a few limitations regarding its structural assumptions. The SCM assumes an Additive Noise Model (ANM). Although ANM is theoretically advantageous for guaranteeing causal identifiability and cleanly decoupling endogenous dynamics from exogenous anomalies for precise root cause localization, it may not capture complex, non-additive external disturbances (e.g., multiplicative noise or nonlinear entanglement) present in reality. Future work will explore flexible non-additive causal mechanisms to further enhance robustness against extreme out-of-distribution (OOD) noise.

NeurIPS Paper Checklist

1. Claims

Question: Do the main claims made in the abstract and introduction accurately reflect the paper’s contributions and scope?

Answer: [Yes]

Justification: The main claims made in the abstract and introduction accurately reflect the paper’s contributions and scope.

Guidelines:

- The answer [N/A] means that the abstract and introduction do not include the claims made in the paper.
- The abstract and/or introduction should clearly state the claims made, including the contributions made in the paper and important assumptions and limitations. A [No] or [N/A] answer to this question will not be perceived well by the reviewers.
- The claims made should match theoretical and experimental results, and reflect how much the results can be expected to generalize to other settings.
- It is fine to include aspirational goals as motivation as long as it is clear that these goals are not attained by the paper.

2. Limitations

Question: Does the paper discuss the limitations of the work performed by the authors?

Answer: [Yes]

Justification: We provide the Limitations in Appendix C.

Guidelines:

- The answer [N/A] means that the paper has no limitation while the answer [No] means that the paper has limitations, but those are not discussed in the paper.
- The authors are encouraged to create a separate “Limitations” section in their paper.
- The paper should point out any strong assumptions and how robust the results are to violations of these assumptions (e.g., independence assumptions, noiseless settings, model well-specification, asymptotic approximations only holding locally). The authors should reflect on how these assumptions might be violated in practice and what the implications would be.
- The authors should reflect on the scope of the claims made, e.g., if the approach was only tested on a few datasets or with a few runs. In general, empirical results often depend on implicit assumptions, which should be articulated.
- The authors should reflect on the factors that influence the performance of the approach. For example, a facial recognition algorithm may perform poorly when image resolution is low or images are taken in low lighting. Or a speech-to-text system might not be used reliably to provide closed captions for online lectures because it fails to handle technical jargon.
- The authors should discuss the computational efficiency of the proposed algorithms and how they scale with dataset size.
- If applicable, the authors should discuss possible limitations of their approach to address problems of privacy and fairness.
- While the authors might fear that complete honesty about limitations might be used by reviewers as grounds for rejection, a worse outcome might be that reviewers discover limitations that aren’t acknowledged in the paper. The authors should use their best judgment and recognize that individual actions in favor of transparency play an important role in developing norms that preserve the integrity of the community. Reviewers will be specifically instructed to not penalize honesty concerning limitations.

3. Theory assumptions and proofs

Question: For each theoretical result, does the paper provide the full set of assumptions and a complete (and correct) proof?

Answer: [Yes]

Justification: We provide the relevant Theory assumptions in Appendix A.

Guidelines:

- The answer [N/A] means that the paper does not include theoretical results.
- All the theorems, formulas, and proofs in the paper should be numbered and cross-referenced.
- All assumptions should be clearly stated or referenced in the statement of any theorems.
- The proofs can either appear in the main paper or the supplemental material, but if they appear in the supplemental material, the authors are encouraged to provide a short proof sketch to provide intuition.
- Inversely, any informal proof provided in the core of the paper should be complemented by formal proofs provided in appendix or supplemental material.
- Theorems and Lemmas that the proof relies upon should be properly referenced.

4. Experimental result reproducibility

Question: Does the paper fully disclose all the information needed to reproduce the main experimental results of the paper to the extent that it affects the main claims and/or conclusions of the paper (regardless of whether the code and data are provided or not)?

Answer: [Yes]

Justification: We provide the implementation details in Experiments 5.1 and Appendix B.4 and the open link <https://anonymous.4open.science/r/PTCD-D4E3> of the data and code in the Appendix B.4.

Guidelines:

- The answer [N/A] means that the paper does not include experiments.
- If the paper includes experiments, a [No] answer to this question will not be perceived well by the reviewers: Making the paper reproducible is important, regardless of whether the code and data are provided or not.
- If the contribution is a dataset and/or model, the authors should describe the steps taken to make their results reproducible or verifiable.
- Depending on the contribution, reproducibility can be accomplished in various ways. For example, if the contribution is a novel architecture, describing the architecture fully might suffice, or if the contribution is a specific model and empirical evaluation, it may be necessary to either make it possible for others to replicate the model with the same dataset, or provide access to the model. In general, releasing code and data is often one good way to accomplish this, but reproducibility can also be provided via detailed instructions for how to replicate the results, access to a hosted model (e.g., in the case of a large language model), releasing of a model checkpoint, or other means that are appropriate to the research performed.
- While NeurIPS does not require releasing code, the conference does require all submissions to provide some reasonable avenue for reproducibility, which may depend on the nature of the contribution. For example
 - (a) If the contribution is primarily a new algorithm, the paper should make it clear how to reproduce that algorithm.
 - (b) If the contribution is primarily a new model architecture, the paper should describe the architecture clearly and fully.
 - (c) If the contribution is a new model (e.g., a large language model), then there should either be a way to access this model for reproducing the results or a way to reproduce the model (e.g., with an open-source dataset or instructions for how to construct the dataset).
 - (d) We recognize that reproducibility may be tricky in some cases, in which case authors are welcome to describe the particular way they provide for reproducibility. In the case of closed-source models, it may be that access to the model is limited in some way (e.g., to registered users), but it should be possible for other researchers to have some path to reproducing or verifying the results.

5. Open access to data and code

Question: Does the paper provide open access to the data and code, with sufficient instructions to faithfully reproduce the main experimental results, as described in supplemental material?

Answer: [Yes]

Justification: We provide the open link <https://anonymous.4open.science/r/PTCD-D4E3> of the data and code in the Appendix B.4.

Guidelines:

- The answer [N/A] means that paper does not include experiments requiring code.
- Please see the NeurIPS code and data submission guidelines (<https://neurips.cc/public/guides/CodeSubmissionPolicy>) for more details.
- While we encourage the release of code and data, we understand that this might not be possible, so [No] is an acceptable answer. Papers cannot be rejected simply for not including code, unless this is central to the contribution (e.g., for a new open-source benchmark).
- The instructions should contain the exact command and environment needed to run to reproduce the results. See the NeurIPS code and data submission guidelines (<https://neurips.cc/public/guides/CodeSubmissionPolicy>) for more details.
- The authors should provide instructions on data access and preparation, including how to access the raw data, preprocessed data, intermediate data, and generated data, etc.
- The authors should provide scripts to reproduce all experimental results for the new proposed method and baselines. If only a subset of experiments are reproducible, they should state which ones are omitted from the script and why.
- At submission time, to preserve anonymity, the authors should release anonymized versions (if applicable).
- Providing as much information as possible in supplemental material (appended to the paper) is recommended, but including URLs to data and code is permitted.

6. Experimental setting/details

Question: Does the paper specify all the training and test details (e.g., data splits, hyperparameters, how they were chosen, type of optimizer) necessary to understand the results?

Answer: [Yes]

Justification: We provide the implementation details in Experiments 5.1 and Appendix B.4.

Guidelines:

- The answer [N/A] means that the paper does not include experiments.
- The experimental setting should be presented in the core of the paper to a level of detail that is necessary to appreciate the results and make sense of them.
- The full details can be provided either with the code, in appendix, or as supplemental material.

7. Experiment statistical significance

Question: Does the paper report error bars suitably and correctly defined or other appropriate information about the statistical significance of the experiments?

Answer: [Yes]

Justification: Each method is run five times with different random seeds, and we report the mean and standard deviation of the evaluation metrics across these runs in Table 3.

Guidelines:

- The answer [N/A] means that the paper does not include experiments.
- The authors should answer [Yes] if the results are accompanied by error bars, confidence intervals, or statistical significance tests, at least for the experiments that support the main claims of the paper.
- The factors of variability that the error bars are capturing should be clearly stated (for example, train/test split, initialization, random drawing of some parameter, or overall run with given experimental conditions).

- The method for calculating the error bars should be explained (closed form formula, call to a library function, bootstrap, etc.)
- The assumptions made should be given (e.g., Normally distributed errors).
- It should be clear whether the error bar is the standard deviation or the standard error of the mean.
- It is OK to report 1-sigma error bars, but one should state it. The authors should preferably report a 2-sigma error bar than state that they have a 96% CI, if the hypothesis of Normality of errors is not verified.
- For asymmetric distributions, the authors should be careful not to show in tables or figures symmetric error bars that would yield results that are out of range (e.g., negative error rates).
- If error bars are reported in tables or plots, the authors should explain in the text how they were calculated and reference the corresponding figures or tables in the text.

8. Experiments compute resources

Question: For each experiment, does the paper provide sufficient information on the computer resources (type of compute workers, memory, time of execution) needed to reproduce the experiments?

Answer: [Yes]

Justification: We provide the implementation details in Appendix B.4.

Guidelines:

- The answer [N/A] means that the paper does not include experiments.
- The paper should indicate the type of compute workers CPU or GPU, internal cluster, or cloud provider, including relevant memory and storage.
- The paper should provide the amount of compute required for each of the individual experimental runs as well as estimate the total compute.
- The paper should disclose whether the full research project required more compute than the experiments reported in the paper (e.g., preliminary or failed experiments that didn't make it into the paper).

9. Code of ethics

Question: Does the research conducted in the paper conform, in every respect, with the NeurIPS Code of Ethics <https://neurips.cc/public/EthicsGuidelines?>

Answer: [Yes]

Justification: We have read the NeurIPS Code of Ethics and confirm that the research conducted in this paper conforms in every respect to the NeurIPS Code of Ethics.

Guidelines:

- The answer [N/A] means that the authors have not reviewed the NeurIPS Code of Ethics.
- If the authors answer [No], they should explain the special circumstances that require a deviation from the Code of Ethics.
- The authors should make sure to preserve anonymity (e.g., if there is a special consideration due to laws or regulations in their jurisdiction).

10. Broader impacts

Question: Does the paper discuss both potential positive societal impacts and negative societal impacts of the work performed?

Answer: [N/A]

Justification: There is no societal impact of the work performed.

Guidelines:

- The answer [N/A] means that there is no societal impact of the work performed.
- If the authors answer [N/A] or [No], they should explain why their work has no societal impact or why the paper does not address societal impact.

- Examples of negative societal impacts include potential malicious or unintended uses (e.g., disinformation, generating fake profiles, surveillance), fairness considerations (e.g., deployment of technologies that could make decisions that unfairly impact specific groups), privacy considerations, and security considerations.
- The conference expects that many papers will be foundational research and not tied to particular applications, let alone deployments. However, if there is a direct path to any negative applications, the authors should point it out. For example, it is legitimate to point out that an improvement in the quality of generative models could be used to generate Deepfakes for disinformation. On the other hand, it is not needed to point out that a generic algorithm for optimizing neural networks could enable people to train models that generate Deepfakes faster.
- The authors should consider possible harms that could arise when the technology is being used as intended and functioning correctly, harms that could arise when the technology is being used as intended but gives incorrect results, and harms following from (intentional or unintentional) misuse of the technology.
- If there are negative societal impacts, the authors could also discuss possible mitigation strategies (e.g., gated release of models, providing defenses in addition to attacks, mechanisms for monitoring misuse, mechanisms to monitor how a system learns from feedback over time, improving the efficiency and accessibility of ML).

11. Safeguards

Question: Does the paper describe safeguards that have been put in place for responsible release of data or models that have a high risk for misuse (e.g., pre-trained language models, image generators, or scraped datasets)?

Answer: [Yes]

Justification: The paper poses no such risks.

Guidelines:

- The answer [N/A] means that the paper poses no such risks.
- Released models that have a high risk for misuse or dual-use should be released with necessary safeguards to allow for controlled use of the model, for example by requiring that users adhere to usage guidelines or restrictions to access the model or implementing safety filters.
- Datasets that have been scraped from the Internet could pose safety risks. The authors should describe how they avoided releasing unsafe images.
- We recognize that providing effective safeguards is challenging, and many papers do not require this, but we encourage authors to take this into account and make a best faith effort.

12. Licenses for existing assets

Question: Are the creators or original owners of assets (e.g., code, data, models), used in the paper, properly credited and are the license and terms of use explicitly mentioned and properly respected?

Answer: [Yes]

Justification: We have properly cited the relevant papers, datasets, and sources in the paper.

Guidelines:

- The answer [N/A] means that the paper does not use existing assets.
- The authors should cite the original paper that produced the code package or dataset.
- The authors should state which version of the asset is used and, if possible, include a URL.
- The name of the license (e.g., CC-BY 4.0) should be included for each asset.
- For scraped data from a particular source (e.g., website), the copyright and terms of service of that source should be provided.
- If assets are released, the license, copyright information, and terms of use in the package should be provided. For popular datasets, paperswithcode.com/datasets has curated licenses for some datasets. Their licensing guide can help determine the license of a dataset.

- For existing datasets that are re-packaged, both the original license and the license of the derived asset (if it has changed) should be provided.
- If this information is not available online, the authors are encouraged to reach out to the asset’s creators.

13. **New assets**

Question: Are new assets introduced in the paper well documented and is the documentation provided alongside the assets?

Answer: [Yes]

Justification: We include detailed documentation in the provided code.

Guidelines:

- The answer [N/A] means that the paper does not release new assets.
- Researchers should communicate the details of the dataset/code/model as part of their submissions via structured templates. This includes details about training, license, limitations, etc.
- The paper should discuss whether and how consent was obtained from people whose asset is used.
- At submission time, remember to anonymize your assets (if applicable). You can either create an anonymized URL or include an anonymized zip file.

14. **Crowdsourcing and research with human subjects**

Question: For crowdsourcing experiments and research with human subjects, does the paper include the full text of instructions given to participants and screenshots, if applicable, as well as details about compensation (if any)?

Answer: [N/A]

Justification: The paper does not involve crowdsourcing nor research with human subjects.

Guidelines:

- The answer [N/A] means that the paper does not involve crowdsourcing nor research with human subjects.
- Including this information in the supplemental material is fine, but if the main contribution of the paper involves human subjects, then as much detail as possible should be included in the main paper.
- According to the NeurIPS Code of Ethics, workers involved in data collection, curation, or other labor should be paid at least the minimum wage in the country of the data collector.

15. **Institutional review board (IRB) approvals or equivalent for research with human subjects**

Question: Does the paper describe potential risks incurred by study participants, whether such risks were disclosed to the subjects, and whether Institutional Review Board (IRB) approvals (or an equivalent approval/review based on the requirements of your country or institution) were obtained?

Answer: [N/A]

Justification: The paper does not involve crowdsourcing nor research with human subjects.

Guidelines:

- The answer [N/A] means that the paper does not involve crowdsourcing nor research with human subjects.
- Depending on the country in which research is conducted, IRB approval (or equivalent) may be required for any human subjects research. If you obtained IRB approval, you should clearly state this in the paper.
- We recognize that the procedures for this may vary significantly between institutions and locations, and we expect authors to adhere to the NeurIPS Code of Ethics and the guidelines for their institution.
- For initial submissions, do not include any information that would break anonymity (if applicable), such as the institution conducting the review.

16. Declaration of LLM usage

Question: Does the paper describe the usage of LLMs if it is an important, original, or non-standard component of the core methods in this research? Note that if the LLM is used only for writing, editing, or formatting purposes and does *not* impact the core methodology, scientific rigor, or originality of the research, declaration is not required.

Answer: [N/A]

Justification: The core method development in this research does not involve LLMs as any important, original, or non-standard components.

Guidelines:

- The answer [N/A] means that the core method development in this research does not involve LLMs as any important, original, or non-standard components.
- Please refer to our LLM policy in the NeurIPS handbook for what should or should not be described.